Journal of Environmental Chemical Engineering 7 (2019) 103214

Contents lists available at ScienceDirect

Journal of Environmental Chemical Engineering

journal homepage: www.elsevier.com/locate/jece

Covalently bonded polyamidoamine functionalized silica used as a Pb(II) scavenger from aqueous solution

Augustus N. Ebelegi[a], Nimibofa Ayawei[a], Donbebe Wankasi[a], Ezekiel D. Dikio[a], Paul N. Diagboya[b,*], Fanyana M. Mtunzi[b]

[a] Department of Chemical Sciences, Niger Delta University, Wilberforce Island, Bayelsa State, Nigeria
[b] Department of Chemistry, Vaal University of Technology, Vanderbijlpark, South Africa

ARTICLE INFO

Keywords:
Generation-3 polyamidoamine dendrimers
Generation-5 polyamidoamine dendrimers
Adsorption
Homogeneous fractal pseudo-second order kinetic model
Thermodynamics
Wastewater treatment

ABSTRACT

Silica was successfully functionalized with generation-3 and 5 polyamidoamine (PAMAM) dendrimers via (3-aminopropyl)triethoxysilane (APTES) linkages to obtain the G3-PAMAM and G5-PAMAM functionalized silica adsorbents designated SG3 and SG5, respectively. The SG3 and SG5 were characterized and explored for Pb(II) removal from aqueous solution. The characterization highlighted successful PAMAM silica synthesis. Preliminary Pb(II) adsorption experiments showed that the SG3 had adsorption efficiency of over 93% compared to pristine silica, silica modified with PAMAM in the absence of the APTES linkage and silica modified with APTES only, each exhibiting ≤1, ≤1 and ≈16% efficiency, respectively. The Pb(II) adsorption equilibria for both adsorbents was 90;min. with optimum adsorption pH of 6 and an experimental adsorption capacities of 121.3 and 132.8;mg/g, respectively. The adsorption process was spontaneous, feasible and endothermic. The adsorption isotherm models suggested Pb(II) ions removal mechanism involving monolayer electrostatic interactions with similar affinity occurring majorly on the SG3 and SG5 surfaces (≈90%) and within the pores (≈10%). The SG3 and SG5 adsorbents exhibited very good reusability even after three adsorption cycles maintaining ≈80% of its adsorption capacity. These fact points to the potential of the SG3 and SG5 adsorbents for removal of Pb(II) from real wastewater.

1. Introdcution

Water pollution by toxic chemical substances has become a challenge worldwide due to the inevitability of water for human, other biota as well as ecosystem survival. Toxic chemical substances have various origins including industries, households, and several intractable sources. The challenge with toxic chemicals in the environment, and within water bodies in particular, stems from the fact that most toxics are persistent and non-biodegradable; thus, they can accumulate in the environment with the possibility of bioaccumulation and toxicity to biota. Toxic effects from chemical substances include diarrhea, nausea, vomiting, hemolysis, neurological and other body system disorders, bone demineralization and death [1,2].

Several toxic chemicals are frequently encountered in water and they include organic [such as polycyclic aromatic hydrocarbons (PAHs), persistent organic pollutants (POPs), dyes, pesticides, emerging pollutants] and inorganic pollutants [such as nitrates, phosphates, chlorides, fluorides, Hg(II), Pb(II), Cr(VI), Cd(II) and As(III)] [3–6]. The toxic inorganic cation Pb(II) is notorious because of its high frequency of occurrence in the environment and the numerous associated health disorders especially in infants: damage to brain, kidney, nervous and reproductive systems [7]. Thus, the need to eliminate Pb(II) from water cannot be overemphasized. Numerous technologies have been proposed for its removal from aqueous solution which include reverse osmosis, ion exchange, chemical precipitation, flocculation, membrane and adsorption-based technologies [8]. However, several techno-economic and environmental drawbacks plague these methods; among them are the need for expert training, high cost of technology and sometimes production of more harmful and environmentally unfriendly by-products. Adsorption-based technologies have exhibited superiority in overcoming these drawbacks and hence they have attracted lots of attention recently [8]. Several adsorbents, including clays [2,9], biomasses and biochar [2,10], porous nanomaterials [11–13], and porous silica materials [14,15], have shown promising results for water treatment. The porous silica materials are especially interesting.

Advances in silica technologies have triggered growing interests in its chemistry due to the ease with which specifically-designed properties can be incorporated into the silica backbone [8,14,15]. The idea of

* Corresponding author.
E-mail address: pauldn2@yahoo.com (P.N. Diagboya).

https://doi.org/10.1016/j.jece.2019.103214
Received 22 March 2019; Received in revised form 12 June 2019; Accepted 13 June 2019
Available online 14 June 2019

synergistic amalgamation of several active molecules or compounds into a larger unit is a successful approach in silica technology for achieving specifically tailored properties, especially in adding desired structural and functional features, in a new material [8]. The focus of this study is to synergistically amalgamate silica gel and polyamidoamine (PAMAM) dendrimers in order to improve the Pb(II) adsorption capacity of silica gel using these PAMAM dendrimers. Though some authors have reported using PAMAM dendrimers for functionalization of silica materials [16–18], it has not been studied on easily obtained silica gel using generation-3 or 5 PAMAM dendrimers combined via covalent linkage.

2. Materials and methods

2.1. Synthesis of G-3 PAMAM functionalized silica

Analytical grade chemicals were used throughout the study. Generation-3 and 5 polyamidoamine (PAMAM) dendrimers with ethylenediamine core, succinic anhydride, (3-aminopropyl)triethoxysilane (APTES), lead nitrate salt and chromatographic grade silica gel (particle size– 240–425 mesh, pore size– 15;nm, pH;–;7, pore volume– 1.15 cm^3/g) were obtained from Sigma Aldrich, while *N*-(3-dimethylaminopropyl-*N'*-ethylcarbodiimide hydrochloride was obtained from Thermo fisher scientific.

The APTES was grafted on the silica gel using similar methods as Acres et al. [19]. Silica gel (30;g) was activated by oven drying at 130;°C for 2;h. Twenty gram of the activated silica gel was refluxed at 115;°C for 6;h in a 10% APTES in 100;mL anhydrous toluene. The product obtained after reflux is the amino-propyl-functionalized silica gel; this was separated from the solution by centrifugation at 4000;rpm for 10;min. The amino functionalized silica gel was washed alternatively with water and ethanol to remove any excess preparation reagents. The last wash was with ethanol followed by oven drying at 105;°C for 1;h. The amino-propyl-functionalized silica was labeled SLC-APTES, and stored in a clean bottle for subsequent use.

Succinic acid terminated generation-3 PAMAM dendrimers were prepared in order to synthesize G-3 or G5 PAMAM functionalized silica (SG3 or SG5) via condensation reaction between the succinic terminal and the amine terminal of the SLC-APTES. The method of Shi et al. [20] was adopted. The succinic acid terminated generation-3 and generation-5 PAMAM dendrimers were prepared by dissolving ≈3.7;mL of G-3 or G-5 PAMAM dendrimers and 3.1;g succinic anhydride in separate 50;mL volumes of dimethyl sulfoxide (DMSO). Both solutions were then transferred into a round bottom flask and refluxed at 80;°C for 12;h and dialyzed with deionized water over 3 d (the deionized water was replaced every 6;h). The succinic acid terminated G-3 or G-5 PAMAM dendrimers were withdrawn from the dialysis setup with a micropipette and stored for further use.

In order to attach the SLC-APTES to the succinic acid terminated generation-3 and 5 PAMAM dendrimers, the method of Jiang et al. [21] was adopted. The SLC-APTES (20;g) and succinic acid terminated PAMAM dendrimers (20;mL) were added into 250;mL round bottom flask containing 75;mL methanol. The coupling agent *N*-(3-dimethylaminopropyl-*N'*-ethylcarbodiimide hydrochloride (EDC) (≈5;mg) [11] was added to the flask and the whole mixture was refluxed at 90;°C for 12;h. The product was separated from the solution by centrifugation at 4000;rpm for 10;min. washed thrice with ethanol and dried at 110;°C for 1;h. The final product is the G-3 PAMAM functionalized silica (SG3). Schematic of the preparation process is shown in Fig. 1.

2.2. Characterization of the adsorbent

The SG3, SG5 and some of the intermediate materials were characterized using Fourier transform infrared (FTIR) spectrometer (Spectrum Two, Perkin Elmer Instruments, USA) in order to determine the associated functional groups, Micromeritics TRISTAR II 3020 analyzer (Micromeritics Instrument Corporation, USA) was used to determine the surface area and porosity, Thermo-gravimetric analyzer (Perkin- Elmer TGA 4000, Perkin Elmer Instruments, USA) was used to obtained the Thermo-gravimetric analysis (TGA) and determine the material stability, and the Scanning Electron Microscope (SEM) (Zeiss Auriga Field Emission) used to determine the surface morphology. The pH at point zero charge (pH_{PZC}) was determined by using the solid addition method; typically the SG3 or SG5 samples (20;mg) were added into 20;mL 0.01;M $NaNO_3$ solutions with pH separately adjusted between 3 and 11. The aliquots were equilibrated by horizontal shaking at 150;rpm for 240;min, followed by pH reading of the aliquots. The pHpzc was obtained from the horizontal intercept of a graph of initial pH versus the difference between the initial and final pH (pH Δ).

2.3. Adsorption study

Lead nitrate salt (Aldrich) was used for the stock solution (1000;mg/L) preparation in this study, while working solutions were subsequently prepared from the stock by serial dilution. Preliminary Pb(II) adsorption studies using pure silica gel (SLC), G-3 PAMAM modified SLC without APTES, SLC-APTES and SG3 were carried out to ascertain the effects of the various treatments on Pb(II) adsorption. Subsequently, adsorption of Pb(II) studies were carried out on the SG3 and SG5 adsorbents to determine the effects of time, pH, concentration and temperature, as well as both adsorbents reusability. The experimental times range from 5 to 240;min, pH from 3 to 7, concentration from 50 to 175;mg/L and temperature from 25 to 45;°C. Except otherwise stated, the equilibrium time used for the study was 90;min (except for effect of time), 20;mg of SG3 or SG5 and 20;mL volume 150;mg/L (except for effect of concentration) of Pb(II) solution. The experiments were carried out in replicate.

For a typical batch experiment, the adsorption was done by adding 20;mg of SG3 or SG5 into 20;mL Pb(II) solution of specified concentration in plastic centrifuge bottles. The SG3/SG5 and 20;mL Pb(II) solution mixtures were placed in an orbital shaker at 200;rpm until equilibrium was attained. The solutions pH was adjusted by either 0.1;M HCl or NaOH when necessary. At equilibrium the plastic centrifuge bottles were withdrawn, followed by centrifugation at 4000;rpm for 10;min. The amount of Pb(II) ions remaining in solution were ascertained using flame atomic absorption spectrophotometer (F-AAS, Shimadzu AA-7000, Japan).

Reusability was carried out using 20;mg of the previously used SG3/SG5. The Pb(II) adsorbed on SG3/SG5 was desorbed by shaking in 20;mL of 0.5;M HNO_3 at 200;rpm for 180;min and then the desorbed Pb (II) analyzed as described above. The SG3/SG5 sample was washed twice with 0.5;M HNO_3 and deionized water before being reused. The reuse was carried out twice more.

2.4. Data management

The amounts of Pb(II) adsorbed on SG3/SG5 were calculated using the equation: $q_e = (C_O - C_e)V/m$; where (C_o) and (C_e) are initial and final concentrations (mg/L), q_e, V and m are the Pb(II) amount of adsorbed (mg/g), Pb(II) solution volume (mL) and SG3/SG5 mass (g), respectively. Three kinetics isotherm models [Lagergren [22] Pseudo-First Order (PFO) (Eq. (1)), Pseudo-Second Order (PSO) (Eq. (2)) and homogeneous Fractal Pseudo-Second Order (FPSO) [9,23] (Eq. (3)) kinetics models, and the Weber-Morris [24] intraparticle diffusion (IPD) (Eq. (4))] were used in describing the effect of time data.

$$q_t = q_e(1 - e^{-k_1 t}) \tag{1}$$

$$q_t = \frac{q_e^2 k_2 t}{1 + q_e k_2 t} \tag{2}$$

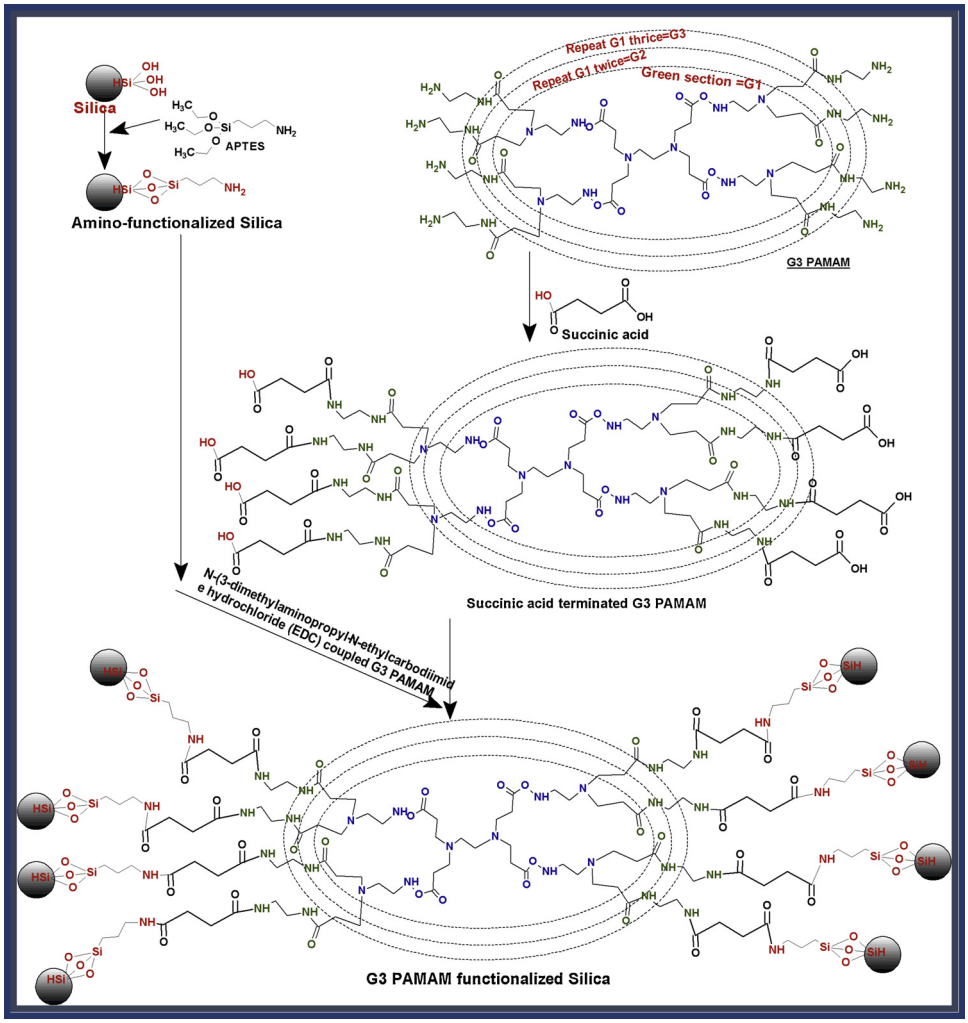

Fig. 1. Schematics for the synthesis of SG3; similar scheme applies to the SG5 adsorbent with the starting PAMAM being a G-5 rather than a G-3.

$$q_t = \frac{k_f q_e^2 t^{\alpha}}{1 + k_f q_e t^{\alpha}} \tag{3}$$

$$q_e = k_{IPD} t^{1/2} + C \tag{4}$$

The symbols q_e and q_t are the amounts of Pb(II) adsorbed (mg/g) on the SG3/SG5 at equilibrium and time t, respectively; and k_1 (/min), k_2 (g/g/min), k_f and k_{IPD} (g/g ;$min^{1/2}$) are the rate constants of the PFO, PSO, FPSO and IPD, respectively; α is the fractional time index, while C (mg/g) is the amount of Pb(II) adsorbed on the SG3/SG5 surfaces. Model parameters were generated from the KyPlot software.

Two adsorption isotherm models [the Langmuir [25] (Eq. (5)) and Freundlich [26] (Eq. (6))] have been employed to describe the equilibrium data.

$$q_e = \frac{Q_O b C^e}{1 + bC_e} \tag{5}$$

$$q_e = k_f C_e^n \tag{6}$$

The parameters Q_o, b, k_f and n are the SG3/SG5 maximum adsorption capacities for Pb(II) per unit weight, energy-related parameter, the Freundlich model capacity factor and the isotherm linearity parameter, respectively.

Thermodynamic [enthalpy change- ΔH^o (Eq. (7)), entropy change- ΔS^o (Eq. (7)) and Gibbs free energy- ΔG^o (Eq. (8))] parameters were also obtained.

$$LnK_o = \frac{\Delta S^o}{R} - \frac{\Delta H^o}{RT} \tag{7}$$

$$\Delta G^o = -RTLnK_o \tag{8}$$

3. Results and discussion

3.1. Physical and chemical characterizations

The schematic synthesis of the G-3/G-5 PAMAM functionalized silica (SG3/SG5) adsorbents is shown in Fig. 1. In order to prepare these adsorbents, the SLC and PAMAM dendrimers were pretreated separately before both were condensed to obtain the final adsorbent. Basically, the APTES was grafted on silica gel via the surface hydroxyl group resulting in the amino (–NH_2) functionalized silica (SLC-APTES). Then the G-3/G-5 PAMAM dendrimers were functionalized with succinic anhydride to obtain the carboxylic acid (−COOH) terminated G-3/G-5 PAMAM dendrimers. Finally, the –NH_2 group of the SLC-APTES and the −COOH group of the succinic acid terminated G-3/G-5 PAMAM dendrimers were combined via an *N*-(3-dimethylaminopropyl-*N*′-ethylcarbodiimide hydrochloride (EDC) [11] assisted coupling reaction resulting in the G-3/G-5 PAMAM functionalized silica (SG3/SG5). The proofs of the successful synthesis of the SG3/SG5 are recorded in results of the physical and chemical properties as shown in Table 1 and Fig. 2. From Table 1, the pH at point of zero charge (pHpzc) values were observed to be low at 3.1 and 2.9, respectively. Thus the SG3 and SG5 surfaces become predominantly negatively charged above these pH

Table 1
Physicochemical parameters of the synthesized SG3 adsorbent.

Adsorbent	pHpzc	BET Surface area (m^2/g)	Pore size (cm^2/g)	Pore width (nm)
SG3	3.1	16.9	0.073	17.4
SG5	2.9	4.7	0.026	22.2

values. The N_2–adsorption/desorption isotherm (not shown) were the classical type IV isotherm, an indication that the SG3 and SG5 were mesoporous; the BET surface area were $\leq$16.9;m^2/g with a relatively large pore width of $\geq$17.4;nm which is higher than that for many reported for silica [27,28]. This large pore widths may create more space for large contaminant molecules to be removed from solution via pore filling [29]. The FTIR spectra of the pristine SLC, SG3 and SG5 adsorbents are shown in Fig. 2a. The characteristic stretching peaks of the silanol Si–O–Si group were obvious at around 1060 and 800;cm^{-1} [29], while the obvious peak associated with the newly added amide group was observed for the SG3 and SG5 at 1630;cm^{-1}.

The TGA spectra are shown in Fig. 2b–d. The spectra showed two major thermal transitions for the pristine SLC, SG3 and SG5 adsorbents as temperature was ramped from 40 to 900;°C. The first was observed below 150;°C for both materials (Fig. 2b and c) and this was attributed to loss of physisorbed water molecules within the interlayer of the backbone silica material [29], resulting in approximately 3.6, 4 and 4% weight losses, respectively. The second thermal transition was observed at 665;°C for SLC with a weight loss of 3.5% (Fig. 2d), while it was observed at a lower temperature (≈560;°C) for SG3 and SG5 with weight losses of ≈4.5% each (Fig. 2c (insert) and d). The higher weight losses exhibited by SG3 and SG5 at lower temperatures were a confirmation of the presence of added APTES and PAMAM dendrimers groups which were more labile than the backbone silica material. Thus the weight losses at this second thermal transition were attributed to the endothermic decompositions of surface hydroxyl groups on the pristine SLC, SG3 and SG5 as well as the APTES and PAMAM groups. The pre- and post-adsorption SG3 and SG5 SEM images were typically similar and are shown in Fig. 2e and f. The Fig. 2e exhibit clear surface images of the pre-adsorption SEM while the post-adsorption surface SEM images showed shinny agglomerated surfaces due to the presence of the adsorbed Pb(II) cations.

Preliminary experiments were carried out to determine the Pb(II) adsorption potential of the pristine SLC, the SLC modified with PAMAM in the absence of APTES, the SLC-APTES and the SG3. The results of the experiments are shown in Fig. 3a. Using experimental adsorbent masses of 20;mg and 20;mL of 50;mg/L Pb(II) solution, it was observed that the pristine SLC and SLC modified with PAMAM in the absence of APTES each had less than 1% Pb(II) adsorption, while the SLC-APTES had ≈16% Pb(II). However, the SG3 exhibited an excellent adsorption compared with these adsorbents with over 93% Pb(II) adsorption. Thus, the SG3 and SG5 Pb(II) adsorption properties were further investigated.

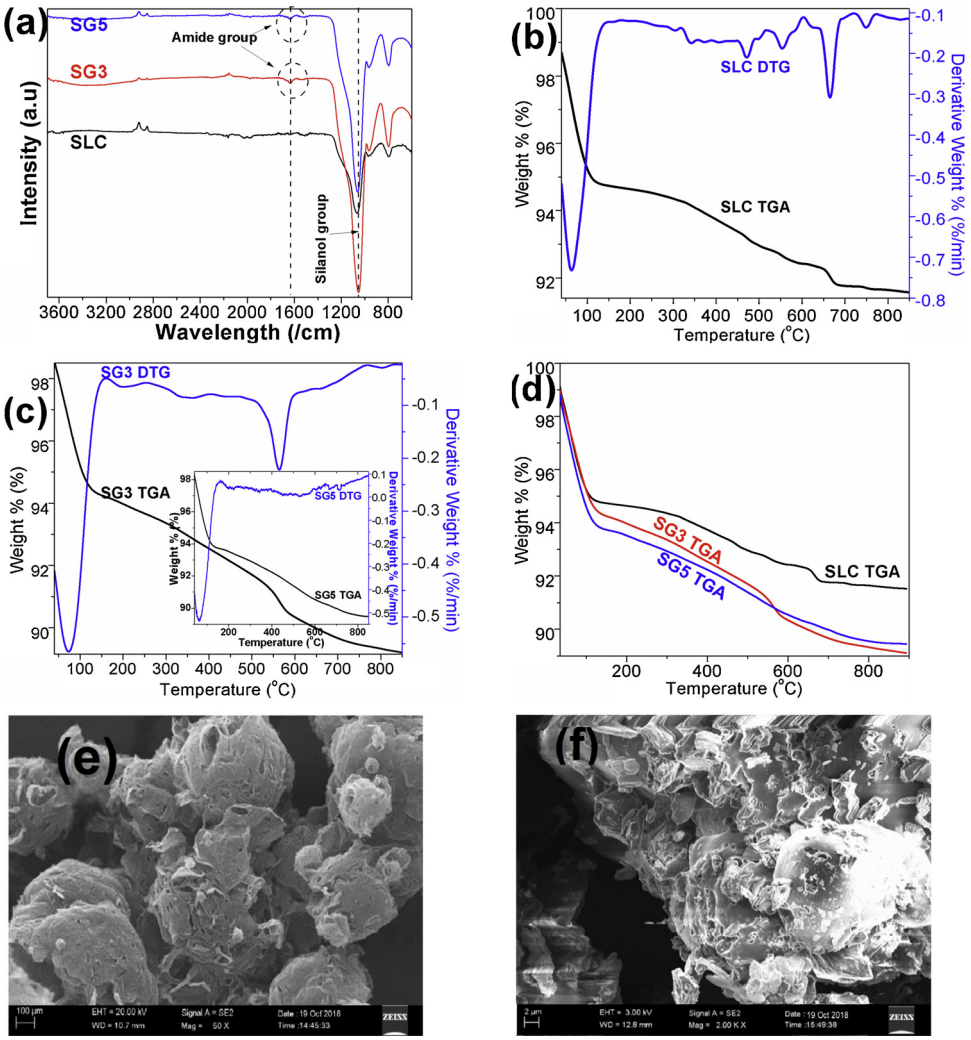

Fig. 2. (a) FTIR spectra of SLC, SG3 and SG5; TGA and DTA spectra of (b) SLC, (c) SG3 (Insert: SG5); (d) comparison of TGA spectra for SLC, SG3 and SG5; SEM micrograph of typical SG adsorbent (e) before and (f) after Pb(II) adsorption.

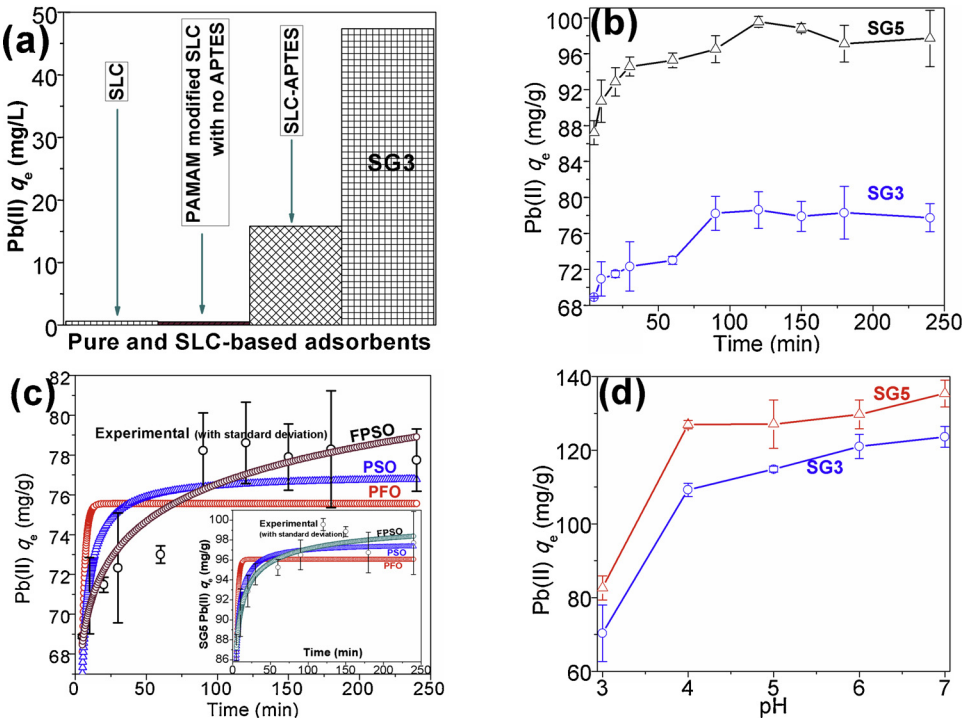

Fig. 3. (a) Preliminary Pb(II) adsorption results using pristine SLC, SLC modified with PAMAM in the absence of APTES, SLC modified with APTES in the absence of PAMAM, and SLC modified with APTES and then PAMAM (SG3); SG3 and SG5 adsorption trends for Pb(II) as (b) time increased; (c) comparison of the pseudo-first, second order kinetic model and the fractal second order kinetic model fittings for SG3 (Insert: SG5); (d) Pb(II) adsorption trend on SG3 and SG5 as pH increased.

3.2. Rate and kinetics of SG3 and SG5 Pb(II) adsorption

Results of Pb(II) adsorption trend on the SG3 and SG5 as time varied are shown in Fig. 3b. From this, it was observed that adsorption rates were very fast at the beginning of the experiment to the initial 90;min when the adsorption-desorption rates became stable and equilibria were achieved. The initial fast adsorption rate was ascribed to adsorption on the numerous vacant surface adsorption sites and filling of the pore spaces by Pb(II) ions in solution. After this point, no more significant Pb(II) adsorption was possible because available adsorption sites have been filled and thus equilibrium is said to have been attained. From these experiments, the time for equilibrium attainment by both SG3 and SG5 was observed to be 90;min. Further, the time data from this particular experiment was fitted to and described using four adsorption kinetic models; the pseudo-first and second order, homogeneous fractal pseudo-second order and the intra-particle kinetic models. The results are shown in Table 2 and Fig. 3c.

The evaluation of the effect of time on Pb(II) adsorption data was carried out by comparing the pseudo–first order and pseudo–second order kinetic models (the nonlinear fittings are shown in Fig. 3c) to the experimental data by using their correlation coefficients (;r^2) and the equilibrium adsorption (q_e) values. It was observed that the ;r^2 value fitting of the pseudo–second order kinetic model was better correlated and predicted the experimental q_e value. Thus, the experimental data fitted the pseudo–second order kinetic model better then the pseudo–-first order kinetic model, and may give insight into the adsorption process. This fitting suggests that the Pb(II) removal mechanism was mainly electrostatic interactions between the Pb(II) ions and the active functional groups on the SG3 and SG5 hybrids [9,30]. However, comparing both models with the homogeneous fractal pseudo-second order kinetic model showed that the later gave better ;r^2 value; implying that the model could also reasonably describe the obtained data with more details. The fractal kinetic model gave the best fit (Table 2 and Fig. 3c) and also indicated a higher Pb(II) uptake rate (k_f) than other models. This high k_f has been reported to be related to faster and higher surface uptake due to high cation exchange capacity [9]. The high correlation of the fractal model to the experimental data suggests a complex process of chemical interactions between adsorbed Pb(II) ions and the functional groups on the SG3 and SG5 surfaces which includes several van der Waals interactions. The intra-particle diffusion kinetic model parameter C (mg/g) gave an indication of the surface and pore adsorption of Pb(II) on the SG3 and SG5 adsorbents. For a C value that is equal to the q_e value, it implied the adsorption was basically a surface phenomenon; but for lower C value, the remaining was attributed to pore adsorption or filling [30]. Thus, the C value in Table 2 implied approximately 90% surface adsorption and 10 % pore filling. The implication of both surface and pore adsorption of Pb(II) on the SG3 and SG5 adsorbents from the intra-particle diffusion kinetic model is that this model is in strong agreement with the fractal pseudo-second order kinetic model; thus the adsorption mechanism may not simply be electrostatic as suggested by the pseudo-second order kinetic model. If this is the case, then the adsorption isotherm model would give further insights on the process.

Table 2
Kinetic model parameters for Pb(II) adsorption.

Kinetic model	Parameter	Pb(II) SG3	Pb(II) SG5
*PFO	q_e (mg/g)	75.6	96.1
	k_1 (/min)	0.46	0.46
	;r^2	0.586	0.758
*PSO	q_e (mg/g)	77.0	97.6
	k_2 (g/mg/min)	0.017	0.015
	;r^2	0.819	0.936
*FPSO	q_e (mg/g)	153.1	101.1
	k_f	0.005	0.030
	α	0.07	0.46
	;r^2	0.942	0.966
	C (mg/g)	68.3	88.9
*IPD	k_i (g/g ;$min^{1/2}$)	0.756	0.724
	;r^2	0.920	0.864
*PPA from IPD	%	12.9	9.2
*PSA from IPD	%	87.1	90.8
Experimental q_e	mg/g	78.4	97.9

*Pseudo-first order (PFO) model; *Pseudo-second order (PSO) model; *Fractal pseudo-second order (FPSO) model; *Intra-particle diffusion (IPD) model; *PPA;=;Predicted pore adsorption from IPD; PSA;=;Predicted surface adsorption from IPD.

3.3. Effect of pH on Pb(II) adsorption on SG3 and SG5

Ascertaining the response of a new adsorbent to aqueous pH variations is vital in predicting the effectiveness of such an adsorbent. It has been reported that pH affects the charge density surrounding the adsorbent as well as the adsorbate; and this ultimately controls the degree of adsorption [10]. Thus, the Pb(II) adsorption trends on SG3 and SG5 as pH varied from 3 to 7 was examined and results showed in Fig. 3d. It was observed that the absorption increased with increase in pH of the aqueous solution. These trends can be explained in terms of the SG3 and SG5 pH values at point of zero charge (pHpzc) which were observed to be 3.1 and 2.9. Below the pHpzc, the SG3 and SG5 adsorption surfaces which are linked to anionic functional groups, including the hydroxyl and carbonates, are blocked by protonation making them uncharged thus Pb(II) ions removal are mainly possible via pore filling with very little electrostatic attraction; this is the reason for the very low adsorption values. However, with increasing pH, these surface adsorption sites become progressively deprotonated and negatively charged. This leads to more electrostatic interactions between the Pb(II) ions in solution and the now charged surface functional groups, and consequently increasingly higher Pb(II) adsorption as observed in Fig. 3d. From the experimental result, optimum adsorption was observed at pH 6 and 5 for SG3 and SG5, respectively.

3.4. Adsorption trends at varying Pb(II) ions and temperature

Results of the effect of varying Pb(II) ion concentrations on SG3 and SG5 adsorption are depicted as the adsorption trend plots in Fig. 4a and b. The trends showed increases in Pb(II) adsorption by SG3 and SG5 as concentration increased from 75 through 175;mg/L. These trends were also observed for the various temperatures investigated: 20, 30 and 40;°C (Fig. 4a and b). Similar trends have been reported by others in literature [2,10,31]. This trend may be attributed to the behaviour of Pb(II) ions between the external surfaces of the SG3 and SG5 and the internal pores. At equilibrium for a particular aqueous concentration when the movement of Pb(II) ions between the SG3 and SG5 surfaces and pores are equal, movement of the ions across both boundaries will be significantly impermissible. However, increasing the aqueous concentration of the Pb(II) ions will re-ignite movement across both boundaries resulting in the observed higher adsorption [2,10].

Table 3
Adsorption isotherm models parameters for Pb(II).

Adsorption isotherm model	Parameter	Pb(II) SG3	Pb(II) SG5
Langmuir	Q_o (mg/g)	125.0	142.9
	β	2.00	3.50
	;r^2	0.997	0.996
Freundlich	n	0.119	0.253
	k_f	83.75	76.03
	;r^2	0.959	0.815
Experimental Q_o (mg/g)		122.1	132.8

In order to better describe the adsorption mechanism, the equilibrium Pb(II) adsorption data on SG3 and SG5 at 40;°C (313;K) were fitted to two adsorption isotherm models: the Langmuir and Freundlich models. Comparison of both model parameters in Table 3 showed that the experimental data fitted the Langmuir adsorption isotherm model better than the Freundlich model. The Langmuir model had a correlation coefficient (;r^2) closer to unity (0.970) than the Freundlich (0.855). The Langmuir was also able to relatively predict the SG3 and SG5 maximum adsorption capacity (Q_o) values of 122.1 and 132.8;mg/g which were closer to the experimental Q_o values for both adsorbents. The correlation of the experimental data to the Langmuir adsorption isotherm model suggests that the adsorption of Pb(II) on SG3 and SG5 might have occurred on sites of equal affinity for the Pb(II) ions and there was only monolayer of Pb(II) ions formed on the SG3 surface at equilibrium [2,32]. This is in contrast to the Freundlich model which assumes that the adsorption of Pb(II) ions occurred on SG3 surfaces of unequal energy with formation of Pb(II) ion multilayer on these surfaces at equilibrium.

However, the relatively high ;r^2 values of the Freundlich isotherm may be explained thus [33,34]: when adsorption occurs in dissimilar sites having approximately equal affinity, they each obey the Langmuir adsorption isotherm model. A combination of these individual

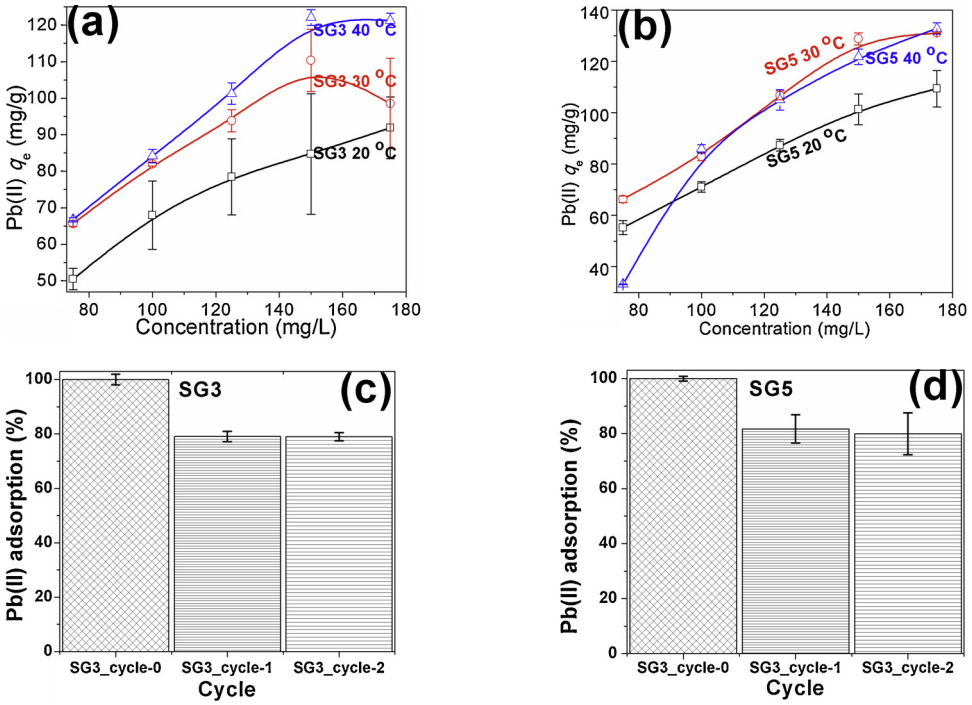

Fig. 4. Effect of temperature on Pb(II) adsorption on (a) SG3, (b) SG5; Reusability studies plots for Pb(II) adsorption on (c) SG3 and (d) SG5 showing three adsorption cycles.

Langmuir isotherms result in close approximation to the Freundlich adsorption isotherm model as observed in Table 3. Also, a critical look at the Freundlich *n* values in Table 3 show that these small values which were less than unity (0.119 and 0.253 for SG3 and SG5, respectively) indicated that the adsorption processes tended towards non–linearity (i.e. more toward the Freundlich than the Langmuir adsorption isotherm). The *n* values may be considered as an index of surface site energy distribution [33]; thus these *n* values suggest adsorption on heterogeneous adsorption sites with slightly unequal affinity for the Pb (II) ions. This reasoning is in congruent with the fractal pseudo-second order kinetic model above which suggested that Pb(II) removal processes involved several van der Waals interactions occurring both on the surface and within the pores of SG3 and SG5 adsorbents.

Increasing the ambient experimental temperature from 20 through 40;°C (Fig. 4a and b) showed that temperature had a positive effect on the adsorption of Pb(II) ions especially on SG3; thus, increasing the temperature, increases Pb(II) adsorption. Some researchers have reported similar trends [30,35]. This trend suggests an endothermic process for Pb(II) ions adsorption on the SG3 and SG5 adsorbents. In order to ascertain this, the adsorption process was evaluated using the thermodynamic parameters (ΔH°, ΔS° and ΔG°) which were calculated from the experimental equilibrum data obtianed at the various temperatures investigated and the parameters are shown in Table 4. The ΔG° values for all temperatures studied were negative, and suggested spontaneous and feasible Pb(II) adsorption processes on the SG3 and SG5. The value of ΔH° obtained from the calculation was positive and this confirmed the assumption that the SG3 and SG5 Pb(II) adsorption processes were endothermic. For a typical endothermic process, increase in external energy input would favour the forward process; thus, the enhanced Pb(II) adsorption with increase in solution temperature [35]. The positive value of the ΔS° is an indication of increased randomness of the Pb(II) ions in solution as the adsorption processes moved towards equilibrium.

3.5. Reusability study and comparison with reported adsorbents

The reusability of the SG3 and SG5 adsorbents were investigated in order to ascertain if their use as a Pb(II) adsorbent is economically beneficial. Three cycles of adsorption results using previously used SG3 and SG5 adsorbents are depicted in Fig. 4b and c. This result showed that the second and third adsorption cycles were slightly lower than the first process by approximately 20%. The higher adsorption recorded for the first SG3 and SG5 adsorption processes were attributed to the empty adsorption sites available on both adsorbent. After the first adsorption process, desorption of the surface adsorbed Pb(II) ions were simple because the desorbing reagent could easily access the surface. However, the Pb(II) ions within the SG3 and SG5 pores or crevices are difficult to access and thus desorption of the ions from these parts and their reuse was impossible. This implies that in the subsequent adsorption cycles, the pores or crevices became inaccessible leading the lowered and nearly constant adsorption capacity recorded.

The SG3 and SG5 adsorption capacity for Pb(II) have been compared with some other silica-based and low-cost materials reported in the literature (Table 5). The comparison showed that both adsorbents performed better than several reported silica-based adsorbents for Pb (II) adsorption, as well as most pristine and composite hybrid low-cost materials reported in the literature. The fact that the adsorption capacity values of both adsorbents were comparable to some of the best performing silica-based adsorbents reported in literature points to the potential of this adsorbent for removal of Pb(II) from real wastewater.

Table 4
Thermodynamic parameters of the SG3 and SG5 adsorbents for Pb(II) adsorption.

Thermodynamic Parameter		Pb(II) SG3	Pb(II) SG5
ΔH°	kJ mol^{-1}	178.52	152.25
ΔS°	J mol^{-1};K^{-1}	627.79	538.75
ΔG° (kJ mol^{-1})	293 K	–4.30	–4.89
	303 K	–14.15	–12.51
	313;K	–16.70	–15.57

Table 5
Comparison of SG3 Pb(II) adsorption capacity with some adsorbents reported in literature.

Adsorbent	q_e (mg/g)	Reference
MWCNT/SiO_2 composite	13	[36]
Carica papaya/Pine cone-Feldspar composite	≈16	[9]
SBA-15-non-imprinted polymer	18.4	[37]
Cobalt Ferrite Magnetic Zn(II)-Silica	≈20	[38]
SBA-15-Pb(II)-imprinted polymer	38.0	[37]
N-[3-(trimethoxysilyl)propyl]-ethylenediamine grafted SLC	38.1	[39]
NH2-MCM-41	57.7	[40]
Magnetized *Quercus robur* biomass/biomass	≈67	[31]
Magnetic core-shell APTES-silica	76.7	[41]
Aminopropyl-SBA-15	97.7	[42]
(2Z)-1-(1,5-dimethyl-1H-pyrazol-3-yl)-3- hydroxybut-2-en-1-one grafted silica gel	94.2	[43]
3-(2-aminoethylamino)propyldimethoxymethylsilane grafted silica spheres	102.7	[44]
SG3	122.1	This study
SG5	132.8	This study
EDTA-Chitosan-TEOS	128.5	[28]
Co-Zn-Al Layer double hydroxide	130.3	[30]
Diethanolamine grafted nanosilica	154.4	[35]
Silica-PAMAM-G2.0	165.8	[17]
EDTA-SBA-15	273.2	[45]

4. Conclusion

Silica was covalently functionalized with generation-3 and 5 polyamidoamine (PAMAM) dendrimers via a (3-aminopropyl)triethoxysilane (APTES) linkage to obtain a G3/G5-PAMAM functionalized silica (SG3/SG5). The SG3 and SG5 were characterized and explored for Pb(II) removal from aqueous solution. The characterizations showed the success of the synthesis due to the presence of FTIR peak associated with amide group (1630;cm^{-1}), larger pore sizes (≥17.4) in comparison to pristine silica and slightly lower thermal stability due to the presence of the incorporated groups, while the post-Pb(II)-adsorption SEM images showed the presence of agglomerated Pb(II) ions on the SG3 and SG5 surfaces. Preliminary Pb(II) adsorption experiments showed that the SG3 had adsorption efficiency of over 93% compared to pristine silica, silica modified with PAMAM in the absence of the APTES linkage and silica modified with APTES only, each exhibiting ≤1, ≤1 and ≈16% efficiency, respectively. Further SG3 and SG5 Pb (II) adsorption experiments showed a fast equilibrium time of 90;min., optimum adsorption pH of 5–6 and experimental Pb(II) adsorption capacity values of 122.1 and 132.8;mg/g, respectively; performances which were better than several silica-based adsorbents and composite hybrid low-cost materials reported in the literature. Experimental data and calculated thermodynamic variables indicated spontaneous (negative ΔG^{o}) and endothermic (positive ΔH^{o}) adsorption processes. The adsorption isotherm modeling parameters suggested Pb(II) ions removal mechanism involving dissimilar affinity monolayer adsorption occurring majorly on the adsorbents surfaces (≈90%) and within the pores (≈10%). The SG3 and SG5 exhibited very good reusability even after the three adsorption cycles maintaining ≈80% of their adsorption capacity values. These facts point to the potential of the both adsorbents for removal of Pb(II) from real wastewater.

Acknowledgment

We acknowledge the Department of Chemistry and Research

Directorate, Vaal University of Technology, Vanderbiljpark, South Africa; Department of Chemical Sciences, Niger Delta University, Wilberforce Island, Nigeria; and the SASOL Research grant (VAT Number: 4430113102).

References

[1] E. Igberase, P. Osifo, A. Ofomaja, Adsorption of metal ions by microwave assisted grafting of cross-linked chitosan beads. Equilibrium, isotherm, thermodynamic and desorption studies, Appl. Organomet. Chem. (2018), https://doi.org/10.1002/aoc.4131.

[2] H.O. Chukwuemeka-Okorie, P.N. Ekemezie, K.G. Akpomie, C.S. Olikagu, Calcined corncob-kaolinite combo as new sorbent for sequestration of toxic metal ions from polluted aqua media and desorption, Front. Chem. 6 (2018).

[3] O.A. Adesina, J.A. Sonibare, P.N. Diagboya, A. Adejuwon, T. Famubode, J.O. Bello, Periodic characterization of alkyl-naphthalenes in stack gas and ambient air around a medical waste incinerator, Environ. Sci. Pollut. Res. 24 (2017) 21770–21777.

[4] M.À. Olivella, P. Jové, A. Oliveras, The use of cork waste as a biosorbent for persistent organic pollutants–Study of adsorption/desorption of polycyclic aromatic hydrocarbons, J Environ. Sci. Heal. A 46 (2011) 824–832.

[5] L.A. Cragin, J.S. Kesner, A.M. Bachand, D.B. Barr, J.W. Meadows, E.F. Krieg, J.S. Reif, Menstrual cycle characteristics and reproductive hormone levels in women exposed to atrazine in drinking water, Environ. Res. 111 (2011) 1293–1301.

[6] D.S. Gamble, The chemistry component of agricultural pesticide regulatory technology, Curr. Opin. Environ. Sci. Health 4 (2018) 16–18.

[7] S.K. Yadav, D.K. Singh, S. Sinha, Chemical carbonization of papaya seed originated charcoals for sorption of Pb(II) from aqueous solution, J. Environ. Chem. Eng. 2 (2014) 9–19.

[8] P.N. Diagboya, E.D. Dikio, Silica-based mesoporous materials; emerging designer adsorbents for aqueous pollutants removal and water treatment, Microporous Mesoporous Mater. 266C (2018) 252–267.

[9] B.I. Olu-Owolabi, P.N. Diagboya, E.I. Unuabonah, A.H. Alabi, R.-A. Düring, K.O. Adebowale, Fractal-like concepts for evaluation of toxic metals adsorption efficiency of feldspar-biomass composites, J. Clean. Prod. 171C (2018) 884–891.

[10] P.N. Diagboya, E.D. Dikio, Scavenging of aqueous toxic organic and inorganic cations using novel facile magneto-carbon black-clay composite adsorbent, J. Clean. Prod. 180 (2018) 71–80.

[11] P.N. Diagboya, B.I. Olu-Owolabi, D. Zhou, B.-H. Han, Graphene oxide–tripolyphosphate hybrid used as a potent sorbent for cationic dyes, Carbon 79 (2014) 174–182.

[12] C.A. Sophia, E.C. Lima, Removal of emerging contaminants from the environment by adsorption, Ecotoxicol. Environ. Saf. 150 (2018) 1–17.

[13] S. Kabiri, D.N.H. Tran, M.A. Cole, D. Losic, Functionalized three-dimensional (3D) graphene composite for high efficiency removal of mercury, Environ. Sci. Water Res. Technol. 2 (2016) 390–402.

[14] R. Kishor, A.K. Ghoshal, APTES grafted ordered mesoporous silica KIT-6 for CO2 adsorption, Chem. Eng. J. 262 (2015) 882–890.

[15] D.Q. Melo, V.O.S. Neto, J.T. Oliveira, A.L. Barros, E.C.C. Gomes, G.S.C. Raulino, E. Longuinotti, R.F. Nascimento, Adsorption equilibria of Cu2+, Zn2+, and Cd2+on EDTA-Functionalized silica spheres, J. Chem. Eng. Data 58 (2013) 798–806.

[16] A. Shahbazi, H. Younesi, A. Badiei, Batch and fixed-bed column adsorption of Cu (II), Pb(II) and Cd(II) from aqueous solution onto functionalised SBA-15 mesoporous silica, Can. J. Chem. Eng. 91 (2013) 739–750.

[17] Y. Niu, R. Qu, C. Sun, C. Wang, H. Chen, C. Ji, Y. Zhang, X. Shao, F. Bu, Adsorption of Pb(II) from aqueous solution by silica-gel supported hyperbranched polyamidoamine dendrimers, J. Hazard. Mater. 244–245 (2013) 276–286.

[18] T. Fu, Y. Niu, Y. Zhou, K. Wang, Q. Mu, R. Qu, H. Chen, B. Yuan, H. Yang, Adsorption of Mn(II) from aqueous solution by silica-gel supported polyamidoamine dendrimers: experimental and DFT study, J. Taiwan Inst. Chem. Eng. 97 (2019) 189–199.

[19] R.G. Acres, A.V. Ellis, J. Alvino, C.E. Lenahan, D.A. Khodakov, G.F. Metha, G.G. Andersson, Molecular structure of 3-aminopropyltriethoxysilane layers formed on silanol-terminated silicon surfaces, J. Phys. Chem. C 116 (2012) 6289–6297.

[20] X. Shi, K. Sun, L.P. Balogh, J.R. Baker Jr., Synthesis, characterization, and manipulation of dendrimer-stabilized iron sulfide nanoparticles, Nanotechnology 17 (2006) 4554.

[21] Y. Jiang, Q. Gao, H. Yu, Y. Chen, F. Deng, Intensively competitive adsorption for heavy metal ions by PAMAM-SBA-15 and EDTA-PAMAM-SBA-15 inorganic–organic hybrid materials, Microporous Mesoporous Mater. 103 (2007) 316–324.

[22] S. Lagergren, Zur theorie der sogenannten adsorption gelöster stoffe, Kungl. Svenska Vetenskapsakad. Handl. 24 (1898) 1–39.

[23] M. Haerifar, S. Azizian, Fractal-like kinetics for adsorption on heterogeneous solid surfaces, J. Phys. Chem. C 118 (2014) 1129–1134.

[24] W.J. Weber, J.C. Morris, Kinetics of adsorption on carbon from solutions, J. Sanit. Engineering Division, Am. Soc. Civil Eng. 89 (1963) 31–60.

[25] I. Langmuir, The constitution and fundamental properties of solids and liquids, J. Am. Soc. Brew. Chem. 38 (1916) 2221–2295.

[26] H.M.F. Freundlich, Über die adsorption in lösungen, Zeitschrift für Physikalische Chemie 57A (1906) 385–470 57A.

[27] Z. Lu, R. Wang, Z. Xia, L. Gong, Experimental investigation adsorption chillers using micro-porous silica gel–water and compound adsorbent-methanol, Energy Convers. Manage. 65 (2013) 430–437.

[28] E. Repo, J.K. Warchoł, A. Bhatnagar, M. Sillanpää, Heavy metals adsorption by novel EDTA-modified chitosan–silica hybrid materials, J. Colloid Interface Sci. 358 (2011) 261–267.

[29] P.N. Diagboya, B.I. Olu-Owolabi, K.O. Adebowale, Microscale scavenging of pentachlorophenol in water using amine and tripolyphosphate-grafted SBA-15 silica: batch and modeling studies, J. Environ. Manage. 146 (2014) 42–49.

[30] C.Y. Abasi, P.N.E. Diagboya, E.D. Dikio, Layered double hydroxide of cobalt-zinc-aluminium intercalated with carbonate ion: preparation and Pb(II) ion removal capacity, Int. J. Environ. Stud. (2018) 1–15.

[31] R.P. Mohubedu, P.N.E. Diagboya, C.Y. Abasi, E.D. Dikio, F. Mtunzi, Magnetic valorization of biomass and biochar of a typical plant nuisance for toxic metals contaminated water treatment, J. Clean. Prod. 209 (2019) 1016–1024.

[32] I.A. Lawal, B. Moodley, Synthesis, characterisation and application of imidazolium based ionic liquid modified montmorillonite sorbents for the removal of amaranth dye, RSC Adv. 5 (2015) 61913–61924.

[33] B.I. Olu-Owolabi, A.H. Alabi, P.N. Diagboya, E.I. Unuabonah, R.A. During, Adsorptive removal of 2,4,6-trichlorophenol in aqueous solution using calcined kaolinite-biomass composites, J. Environ. Manage. 192 (2017) 94–99.

[34] B.I. Olu-Owolabi, P.N. Diagboya, K.O. Adebowale, Evaluation of pyrene sorption–desorption on tropical soils, J. Environ. Manage. 137 (2014) 1–9.

[35] C. Xiong, S. Wang, W. Sun, Y. Li, Selective adsorption of Pb(II) from aqueous solution using nanosilica functionalized with diethanolamine: equilibrium, kinetic and thermodynamic, Microchem. J. 146 (2019) 270–278.

[36] T.A. Saleh, Nanocomposite of carbon nanotubes/silica nanoparticles and their use for adsorption of Pb(II): from surface properties to sorption mechanism, Desalin. Water Treat. 57 (2016) 10730–10744.

[37] Y. Liu, Z. Liu, J. Gao, J. Dai, J. Han, Y. Wang, J. Xie, Y. Yan, Selective adsorption behavior of Pb(II) by mesoporous silica SBA-15-supported Pb(II)-imprinted polymer based on surface molecularly imprinting technique, J. Hazard. Mater. 186 (2011) 197–205.

[38] H. Rong, L. Weiming, D. Dayi, C. Wensen, L. He, W. Chaohai, T. Youwen, Efficient removal of lead from highly acidic wastewater by periodic ion imprinted mesoporous SBA-15 organosilica combining metal coordination and co-condensation, J. Mater. Chem. A 3 (2015) 9789–9798.

[39] N. Chiron, R. Guilet, E. Deydier, Adsorption of Cu(II) and Pb(II) onto a grafted silica: isotherms and kinetic models, Water Res. 37 (2003) 3079–3086.

[40] A. Heidari, H. Younesi, Z. Mehraban, Removal of Ni(II), Cd(II), and Pb(II) from a ternary aqueous solution by amino functionalized mesoporous and nano mesoporous silica, Chem. Eng. J. 153 (2009) 70–79.

[41] J. Wang, S. Zheng, Y. Shao, J. Liu, Z. Xu, D. Zhu, Amino-functionalized Fe3O4@SiO2 core–shell magnetic nanomaterial as a novel adsorbent for aqueous heavy metals removal, J. Colloid Interface Sci. 349 (2010) 293–299.

[42] J. Aguado, J.M. Arsuaga, A. Arencibia, M. Lindo, V. Gascón, Aqueous heavy metals removal by adsorption on amine-functionalized mesoporous silica, J. Hazard. Mater. 163 (2009) 213–221.

[43] S. Tighadouini, S. Radi, M. Bacquet, S. Degoutin, M. Zaghrioui, S. Jodeh, I. Warad, Removal efficiency of Pb(II), Zn(II), Cd(II) and Cu(II) from aqueous solution and natural water by ketoenol–pyrazole receptor functionalized silica hybrid adsorbent, Sep. Sci. Technol. 52 (2017) 608–621.

[44] Z. Zhu, Preparation and characterization of functionalized silica spheres for removal of Cu(ii), Pb(ii), Cr(vi) and Cd(ii) from aqueous solutions, RSC Adv. 5 (2015) 28624–28632.

[45] J. Huang, M. Ye, Y. Qu, L. Chu, R. Chen, Q. He, D. Xu, Pb (II) removal from aqueous media by EDTA-modified mesoporous silica SBA-15, J. Colloid Interface Sci. 385 (2012) 137–146.